Journal Name

ARTICLE

Formic acid oxidation on platinum electrodes: A detailed mechanism supported by experiments and calculations on well-defined surfaces

A. Ferre-Vilaplana,[a,b] J.V. Perales-Rondón,[c] C. Buso-Rogero,[c] J. M. Feliu,[c] and E. Herrero*[c]

In spite of that the formic acid oxidation reaction on electrode surfaces has been extensively investigated, a detailed mechanism explaining all the available experimental evidences on platinum has not been yet described. Herein, using a combined experimental and computational approach, the key elements in the mechanism of the formic acid oxidation reaction on platinum have been completely elucidated, not only for the direct path, through an active intermediate, but also for the CO formation route. Experimental results suggest that the direct oxidation path on platinum takes place in the presence of bidentate adsorbed formate. However, the results reported here provide evidence that this species is not the active intermediate. Monodentate adsorbed formate, whose evolution to the much more favorable bidentate form would be hindered by the presence of neighboring adsorbates, has been found to be the true active intermediate. Moreover, it is found that adsorbed formic acid would have a higher acid constant than in solution, which suggests that adsorbed formate can be originated not only from solution formate but also from formic acid. The CO formation path on platinum can proceed, also from monodentate adsorbed formate, through a dehydrogenation process toward the surface, during which the adsorbate transitions from a Pt—O adsorption mode to a Pt—C one, to form carboxylate. From this last configuration, the C—OH bond is cleaved, on the surface, yielding adsorbed CO and OH. The results and mechanisms reported here provides the best explanation for the whole of the experimental evidences available to date about this reaction, including pH, surface structure and electrode potential effects.

Introduction.

The formic acid oxidation reaction (FAOR) on platinum has been extensively investigated, being an important topic in fuel cells science and technology. First, formic acid can be used as a fuel, with some advantages with respect to hydrogen, such as easier storage and handling. Additionally, FAOR, in which only two electrons are exchanged, can be used as a model reaction to better understand oxidation processes of more complex fuels, such as methanol and ethanol. On the other hand, platinum has been found to be one of the pure metals most active toward the considered reaction. Thus, in order to optimize the electrocatalysis of these small molecules used as fuels, it would be useful if the detailed mechanism of FAOR on platinum was completely elucidated.

The simplest oxidation reaction in which only two electrons are exchanged is that of hydrogen. Its mechanism, which involves the cleavage of a single H—H bond, has been described as the combination of a Heyrovsky or Tafel step (depending on the electrode surface and potential) with one or two Volmer steps, respectively. The complete FAOR, yielding CO_2, also comprises the transfer of two electrons, but this oxidation reaction implies the cleavage of not one but two bonds: a C—H and a O—H bond. Because the O—H bond is involved in an acid-base equilibrium, this splitting can be regarded as an easy step. However, it is generally assumed that, for the C—H bond cleavage a surface site assisting in this process is required, for which platinum surfaces are very active. Despite the apparent simplicity of the sketched reaction, after forty years of research, a detailed and complete mechanism explaining all the available experimental evidences about FAOR on platinum has not been yet described. A reason for that would be that the FAOR mechanism on platinum electrodes is actually more complex than this simple reaction scheme.

Early experiments regarding FAOR on platinum revealed the formation of an adsorbed species, which was difficult to oxidize, reason why it was termed as poison.[1] This species was identified as CO by means of IR spectroscopy.[2] The presence of adsorbed CO pointed out the existence of a reaction path that involves the cleavage of the C—H and C—OH bonds. CO formation represents a problem in the oxidation mechanism. On the one hand, CO is strongly adsorbed on platinum. On the other hand, the oxidation of adsorbed CO requires of an

[a.] *Instituto Tecnológico de Informática, Ciudad Politécnica de la Innovación, Camino de Vera s/n, E-46022 Valencia, Spain.*
[b.] *Departamento de Sistemas Informáticos y Computación, Escuela Politécnica Superior de Alcoy, Universidad Politécnica de Valencia, Plaza Ferrándiz y Carbonell s/n, E-03801 Alcoy, Spain.*
[c.] *Instituto de Electroquímica, Universidad de Alicante, Apdo 99 E-03080, Alicante, Spain. E-mail: herrero@ua.es*

additional oxygen group and the formation of an extra C—O bond. As a result, the oxidation of CO on platinum takes place only at high overpotentials. It could have been possible that FAOR on platinum occurred only through CO as intermediate, but a dual path mechanism was proposed from the initial studies.[3, 4] Under the dual path mechanism model, one path, named the direct path, goes through an active intermediate, meanwhile the other one give rise to adsorbed CO as a relatively inert intermediate. The confirmation of the existence of the direct route came in studies using labeled species and Differential Electrochemical Mass Spectroscopy (DEMS).[5, 6] However, the identification of the active intermediate species involved in the direct path has been much more elusive, probably due to the inherent difficulties of identifying short-lived species buried in the water-electrode interface. Bidentate adsorbed formate (with the two oxygen atoms bounded to the platinum surface) was initially proposed as the active intermediate,[7-10] although its role in the mechanism has been a controverted topic to date.[11-13] Moreover, the disjunctive between formic acid or formate as the species from which FOAR would be initiated, and the mechanism giving rise to CO, have been also subjects of discussion.[14-17]

An additional difficulty to understand FAOR on platinum is the fact that the reaction is very sensitive to the surface structure of the electrode, namely, reaction rates for both paths strongly depend on the arrangements of the surface atoms.[18, 19] Thus, the observed reactivity for a polycrystalline surface is a complex function of the one exhibited by each type of site present in the surface. It is possible that the observed reactivity was dominated by the processes taking place on a specific type of site, masking the reactivity of the remaining sites. Therefore, to reliably establish the reaction mechanism, the strategy of using different single crystal electrodes as model surfaces seems essential. The initial studies focused on the low index planes, namely Pt(111), Pt(110) and Pt(100) surfaces, which contain a single type of site in a 2D periodic arrangement. However, by considering also stepped surfaces, in which the infinite arrangements of the low index planes are perturbed by the presence of steps with different symmetry, additional understanding about the investigated reaction can be obtained. By using different single crystal electrodes, the reactivity of each site can be not only determined, but also experimental and computational results on these model surfaces can be more easily compared. A combined experimental and computational approach is probably the only one that can completely elucidate the FAOR mechanism on platinum.

Assuming the dual path mechanism model, in this article, we will propose a complete and detailed FAOR mechanism, comprising both the direct path and the CO formation route, capable of explaining all the available experimental evidences on platinum. New experiments on well-defined surfaces has been specifically designed to address outstanding problems under extreme conditions (e.g. using highly acidic solutions), and new DFT calculations have been performed searching for insights about mechanisms. With this strategy, the initial specie, the active intermediate and the role played by

bidentate adsorbed formate, and the interfacial pH, surface structure, and electrode potentials effects in the FAOR mechanism on platinum, will be all elucidated. Starting with a critical review of the state of the art, the new experimental and computational results will be presented, concluding with the proposed reaction model. The insights provided in this work are expected to help in the design of better electrocatalysts for FAOR and in the understanding of the oxidation of more complex fuels.

Methods.

Experimental methods.

Details about the electrochemical experiments have been published elsewhere.[17, 20, 21] In brief, platinum single crystal electrodes were oriented, cut and polished from small single crystal beads (ca. 2.5 mm diameter) following the procedure described by Clavilier.[22, 23] The electrodes were cleaned by flame annealing, cooled down in H_2/Ar and protected with water in equilibrium with this atmosphere. Experiments were carried out in a classical two-compartment electrochemical cell deaerated by using Ar (N50, Air Liquide in all gases used), including a large platinum counter electrode and a reversible hydrogen (N50) electrode (RHE) as reference. For the temperature-controlled experiments, the electrochemical cell was immersed in a water bath. Temperature dependent measurements were conducted in a range between 278 and 333 K, using 5 K intervals. In the temperature dependent measurements, the reference electrode was kept at room temperature (298 K), and the direct potential reading was corrected for the thermodiffusion potential using the procedure explained in reference [24]. Solutions were prepared from sulfuric acid, perchloric acid, sodium perchlorate, formic acid (Merck suprapur in all cases) and ultrapure water from Elga.

The potential program for the pulse voltammetry, which allowed obtaining the current transients, was generated with an arbitrary function generator (Rigol, DG3061A) together with a potentiostat (eDAQ EA161) and a digital recorder (eDAQ, ED401). To avoid any interference of the diffusion of formic acid or interfacial pH change in the reaction rate, stationary conditions were attained by using a hanging meniscus rotating disk (HMRD) configuration at 900 rpm (controlled by a Radiometer CTV 101). Full experimental details on the pulsed voltammetry can be found in reference.[25] In summary, the potential program consists in a series of steps between an upper potential (0.9 V for T<298 K and 0.85 V for T≥298 K) to oxidized the accumulated CO in the previous step on the surface and the different sampling potentials. The duration of the steps was always 1 s.

Computational methods.

All DFT calculations were carried out using numerical basis sets,[26] semicore pseudopotentials[27] (which include scalar relativistic effects) and the RPBE functional[28] as implemented in the Dmol3 code.[29] Implicit solvation effects were taken into

account by the COSMO model.[30] Moreover, hydrogen bonds to solvent were captured by means of the inclusion of explicit water molecules in the model when it was considered convenient. The effects of non-zero dipole moments in the supercells were cancelled by means of external fields.[31] Additionally, the relevant transition states were confirmed estimating minimum energy reaction paths between reactants and products by means of the nudged elastic band method.[32] Redox potential effects, when considered, were included in the calculations by means of the computational hydrogen electrode formalism.[33] Finally, molecular dynamic simulations were run under the NVT thermodynamic ensemble.

For direct path calculations, because neutral and charged conditions were considered and compared, the Pt(100) surface was modeled by means of a periodic supercell comprising six layers of metal atoms (48 Pt atoms) and a vacuum slab of 20 Å. The two most internal metal layers were frozen in their bulk crystal locations. The remaining four metal layers were allowed to relax jointly with the adsorbates. The shortest distance between periodic images was 5.71 Å. However, for CO formation path calculations, only neutral charge conditions were considered, and thus four layers of metal atoms with a vacuum slab of 20 Å were considered enough for the models. So, the Pt(111), Pt(100), and Pt(553) surfaces were modeled by 36, 36 and 56 platinum atoms, respectively. For each case, the bottom two layers of metal atoms were frozen in their bulk crystal locations. The remaining two metal layers were allowed to relax jointly with the adsorbates. The shortest distance between periodic images was 8.49 Å, for the three cases.

Optimal configurations (adsorbent/adsorbate, reactants, products and transition states) were sought using numerical basis sets of double-numerical quality. During this phase of the calculations, Brillouin zones were sampled under the Monkhorst-Pack method[34] using grids corresponding to distances in the reciprocal space of the order of 0.02 1/Å and 0.05 1/Å, for the direct path and the CO formation calculations, respectively. Meanwhile convergence was facilitated introducing 0.005 and 0.002 Ha of thermal smearing for the direct path and the CO formation calculations, respectively. Assuming the previously optimized configurations, binding energies, reaction energies and barriers were all estimated using numerical basis sets of double-numerical quality plus polarization. For the CO formation path calculations, Brillouin zone grids were refined to distances of the order of 0.04 1/Å. Energies were extrapolated to 0 K.

Results and discussion

Direct oxidation path.

Role of bidentate adsorbed formate and identification of the active intermediate. Although, for the direct path of FAOR on platinum, several active intermediates were initially proposed, no species different from adsorbed CO was identified in the reaction until Surface Enhanced Infrared Adsorption

Spectroscopy in Attenuated Total Reflection configuration (ATR-SEIRAS) was employed.[7-10] Using a polycrystalline platinum electrode deposited on the IR prism, adsorbed formate was detected. The species was found to be adsorbed in a bidentate configuration, with the two oxygen atoms bounded to the platinum surface. Since the potential region in which the species was detected coincided with the potential region where the direct oxidation takes place, it was proposed as the active intermediate. Thus, the situation would be then rather simple: formic acid is first adsorbed on the surface, as bidentate formate, losing the acid proton from the O—H group. Then, from this configuration, the species evolves to yield CO_2 by breaking the C—H bond. However, a weakness of the described model is that it is not obvious how the C—H bond is broken when formate is adsorbed in bidentate form. So, to further understand the mechanism, additional results should be considered.

As aforementioned, a difficulty with polycrystalline samples is that different routes could simultaneously operate, at different rates on different sites, preventing a correct identification of the mechanism. Thus, studies with single crystal electrodes are more convenient. The problem is that the ATR-SEIRAS technique cannot be applied to single crystal electrodes, because it is not possible to deposit ordered layers on the IR prisms. Unfortunately, all the deposits have a polycrystalline structure. On the other hand, conventional FTIR on single crystal electrodes is not sensitive enough to detect de formation of adsorbed formate. Thus, an alternative approach should be employed to detect the presence of adsorbed intermediates on single crystal electrodes, other than CO. In order to identify the elusive active intermediate, the ideal electrode from all the possible surfaces is probably the Pt(111) electrode. As will be shown later, on this electrode CO is formed exclusively on defects, reason why high quality Pt(111) surfaces are almost not affected by the formation of CO. So, using this electrode and fast voltammetry at scan rates above 20 V s^{-1} in the presence of formic acid, it was possible to detect an adsorbed species on the Pt(111) electrode in perchloric acid solutions.[35] Based on the results for the polycrystalline electrode and on the adsorption modes of acetic acid on Pt(111) electrodes,[36] it was proposed that the adsorbed species was bidentate formate. Also in this case, the onset of adsorption matched that of the direct oxidation, which suggests, once more time, that bidentate adsorbed formate would be the active intermediate.

However, other results insinuated that situation was more complicated that the initially proposed.[11-13] The kinetic analysis of the results of the ATR-SEIRAS experiments coupled with the DEMS technique suggested that bidentate adsorbed formate was not the active intermediate. Recently, a detailed analysis of spectroscopic data also revealed that the measured currents were not proportional to the adsorbed coverage, which reinforced the idea that bidentate adsorbed formate would not be the true active intermediate.[37] These evidences are also present in studies with single crystal electrodes. For the Pt(111) surface, the presence of adsorbed bisulfate (or other anions such as acetate) had small positive effect on the

oxidation of formic acid. In the presence of 0.5 M sulfuric acid solutions, the onset of the oxidation shift slightly to lower overpotential values, which suggests a positive effect of the adsorbed bisulfate.[38] This is a strange result, since the adsorption strength of formate and bisulfate are similar (they adsorb in similar potential ranges on platinum), and thus the high concentration of sulfuric acid should prevent the adsorption of bidentate formate. If bidentate formate is not adsorbed and this is the active intermediate, smaller currents should have been detected. This is, for instance, the situation found in the oxidation of methanol, where a drastic diminution of the currents is observed in sulfuric acid solutions in comparison with the situation found in perchloric acid.[39] These results would imply that bidentate adsorbed formate would not be the active intermediate.

On the other hand, DFT calculations indicates that the cleavage of the C—H bond from adsorbed formate in bidentate form requires a high activation energy, which would make this process very difficult.[40] It has been also found that when a formic acid molecule approaches the surface with the C—H bond pointing towards the surface, the C—H bond cleavage has a negligible energy barrier.[41] However, if this is the only requirement, any metal with dehydrogenation properties (such as Pt or Pd) would have excellent properties for the reaction, with no additional need of further catalysis. However, modification of the Pt surface with some adatoms, such as bismuth, increases the catalytic response.[20, 42] The catalysis of FAOR on adatom-modified Pt(111) electrodes has been explained starting from formate adsorbed on the adatom in monodentate form, evolving to a configuration in which the C—H bond is oriented towards the surface, were the C—H bond cleavage is facilitated by the presence of a neighboring platinum atom. Thus, it can be concluded that the catalysis requires some species that facilitates the interaction of the species in the right configuration, and the pure metal is not enough to achieve highest activity.

Considering the aforementioned evidences and results, the fast voltammetry experiments on the Pt(111) electrode were reanalyzed.[38] From the experiments, it is clear that FAOR on the Pt(111) surface takes place in the presence of an adsorbed species (bidentate adsorbed formate, adsorbed sulfate or adsorbed acetate), and that the onset of the adsorption of these species matches the onset for the oxidation. Then, it can be proposed that these adsorbed species facilitate the adsorption of formate in the right configuration, with the C—H bond to the surface. Thus, the process requires the presence of adsorbed anions (bidentate formate or sulfate) and a least two free platinum sites, one where the incoming species adsorbs, and one where the C—H bond is cleaved. The mechanism is similar to a Langmuir-Hinselwood (L-H) mechanism. In a true L-H mechanism, both adsorbed species react, but in this case one of them (the previously adsorbed formate or anion) only facilitates the adsorption of the second one in the right configuration. Assuming this mechanism model and the bidentate adsorbed coverages calculated from the fast voltammetry experiments, it was possible to reproduce the voltammetric currents measured for a Pt(111)

electrode in perchloric acid solution. The current obtained in voltammetry is, then, proportional to the anion (formate) coverage (θ_A), the number of free sites ($1-\theta_A$), and the kinetic constant, whose value is modulated by the electrode potential with the usual Tafel relationship with α as the transfer coefficient: [38]

$$j \propto k \exp\left(\frac{\alpha FE}{RT}\right)\theta_A\left(1-\theta_A\right) \qquad (1)$$

It should be mentioned that in the equation, the order for the term related to the presence of adsorbed bidentate formate on the surface, (θ_A), is one, not two, as could have been expected because the bidentate nature of the adsorption mode. The rate determining step (rds) is taking place in a free site ($1-\theta_A$), where the neighboring adsorbed formate facilitates the adsorption of the incoming species in the right configuration. Thus, reaction order for adsorbed formate is one because the relevant element for the reaction to occur is that one adsorbed species is required, not the number of sites of the surface occupy by the species.

The initial increase in the currents observed in the voltammetry can be associated with the initial adsorption of bidentate formate, which would facilitate the adsorption of formate in the right configuration, and the increase of the reaction rate with the electrode potential. From the peak potential, current diminishes due to the diminution of free platinum sites where species can react, since the reaction is completely inhibited when formate species block the surface. Thus, it can be concluded that bidentate adsorbed formate is not the true active intermediate, but a facilitating species, corroborating the initial proposal by Behm and col.[11, 12]

To further investigate the FAOR mechanism on platinum, kinetic data for both reaction paths are required, so that the different alternatives for the oxidation mechanism could be confirmed or discarded. For such a purpose, pulsed voltammetry was used.[43, 44] A series of pulses to the desired potential was intercalated between pulses at 0.85 V. During the pulse at 0.85 V, the adsorbed CO species accumulated on the surface are completely oxidized, so that the kinetics of the FAOR can be studied in a subsequent pulse on a surface initially free of CO. Additionally the forced convection during the measurements in the HMRD configuration restores the pH and formic acid concentration in the interphase to the nominal values, assuring that the actual conditions in the interphase are equal to those of the bulk solution. From the oxidation transient measured at the desired potential, and using an appropriate model for the analysis of the data, two important parameters and its dependence with the electrode potential were determined for the two reaction paths, that is: the current density for the active path in the absence of CO, the so called intrinsic activity (the extrapolated current in the transient at t=0), and the CO formation rate. The obtained currents , for the active intermediate reaction path on the different low index planes were Pt(100)>Pt(110)>Pt(111).[25, 45] Additionally, the activity of the different steps was determined, which helped in the understanding of the reactivity of Pt nanoparticles.[46]

The intrinsic activity not only allowed the determination of the true activity for the direct path of the different sites in the surface, but also, and more important, it enables to extract apparent activation energies from its dependence with the temperature.[21, 38] As can be seen in Fig. 1, the apparent activation energy has a complex dependence with the electrode potential. For a simple outer sphere oxidation reaction, the true activation energy should diminish with the electrode potential, according to the Tafel slope. However, in perchloric acid solutions, the apparent activation energy is almost constant in the region between 0.3 and 0.7 V, indicating the presence of kinetic complications in the reaction. It should be stressed that the determined apparent activation energy contains not only the true activation energy of the reaction, but also other factors, such as the effect of the temperature on the formate coverage, according to equation (1). At the onset for the oxidation on platinum single crystal electrodes, the activation energy is relatively low, ca. 50 kJ mol^{-1}. Because the calculated activation energy for the cleavage of the C—H bond in the bidentate configuration is significantly higher (above 1 eV), this value clearly suggests that the scission of the C—H bond occurs from the monodentate adsorbed configuration.
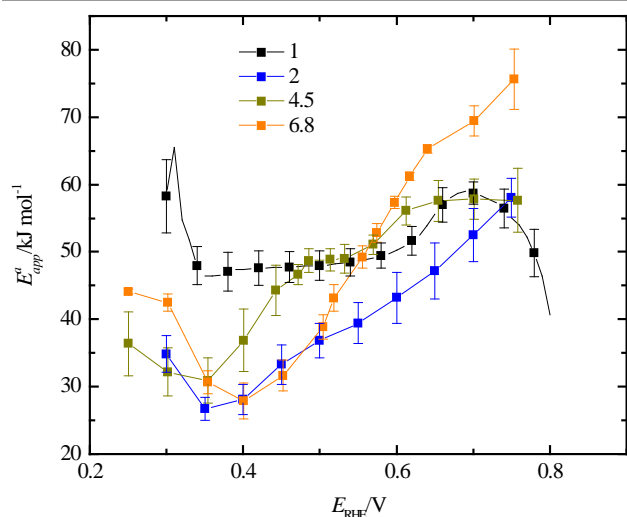

Fig. 1. Apparent activation energy for the oxidation of 0.1 M HCOOH on Pt(111) electrodes in 0.1 M HClO4 (pH=1) and different mixtures of HClO$_4$ and NaClO$_4$ with different pH values.

pH effect and initial species of FAOR. The pK$_a$ of formic acid is 3.75. Thus, for pH<3.75, the global oxidation reaction is

$$HCOOH \leftrightarrow CO_2 + 2H^+ + 2e^- \tag{2}$$

and thus, the equilibrium potential shifts 59 mV per pH unit, as the RHE scale does. However, in the region where pH>3.75, since the major species in solution is formate, the reaction is then:

$$HCOO^- \leftrightarrow CO_2 + H^+ + 2e^- \tag{3}$$

with the equilibrium potential shifting 40 mV per pH unit. Moreover, given that not only formic acid but also formate are present in the solution, whose relative concentrations depend

on the pH, FAOR could be initiated from formic acid or formate.

To determine the initial reactive species of FAOR, formic acid or formate from the solution, pH dependent studies have been carried out by different authors on polycrystalline electrodes. It has been shown that, in the absence of specific adsorption, peak current densities recorded in cyclic voltammetry increase with pH up to a value of 4.[14-17] From that pH value, current remains constant up values close to 10, where the reaction is completely inhibited.[16, 17] Note that phosphate buffered solutions cannot be used in these studies, due to the strong adsorption of phosphate species on the platinum surface at neutral conditions. Unlike the effect of sulfate or acetate, the presence of adsorbed phosphate in neutral solutions strongly affects the reactivity, causing the inhibition of the reaction for pH>5.[16]

A similar behavior the one described above can be observed on single crystal electrodes. Fig. 2 shows the intrinsic activity measured on the Pt(111) surface, at different pH values, using mixtures of perchloric acid and perchlorate to fix the pH. To maintain the interfacial pH, a hanging meniscus rotating disk configuration has been used. As can be seen, the observed behavior for the intrinsic activity on this single crystal electrode is the same as that observed for the peak currents in polycrystalline electrodes, that is, the activity increases up to pH 4, and from this pH value the activity remains constant. This behavior suggests that the rds is a concerted proton-electron transfer.[47, 48]
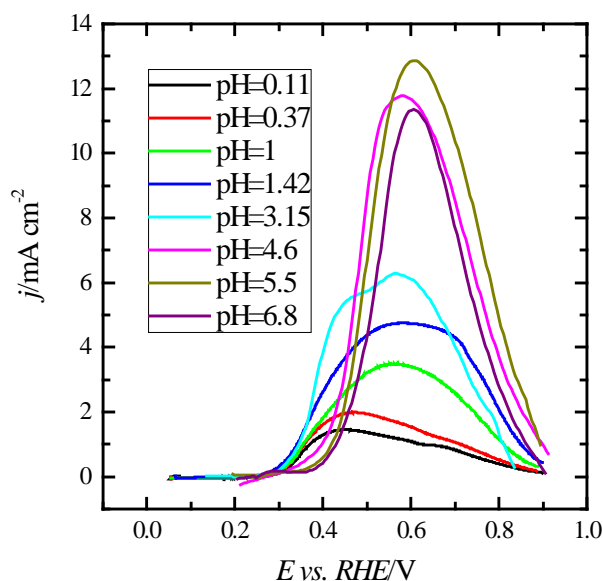

Fig. 2. Intrinsic activity measured for the direct oxidation path for 0.1 M HCOOH solutions in different mixtures of HClO$_4$ and NaClO$_4$ with different pH values for the Pt(111) electrode.

Additional information can be obtained from the onset potential for the reaction. In the RHE scale, the onset potential is constant for pH<4 and then shifts to higher values. If the onset is dependent on the initial adsorption of formate, for pH<3.75, the surface reaction is

$$Pt + HCOOH \leftrightarrow Pt\text{-}OOCH + H^+ + e^- \tag{4}$$
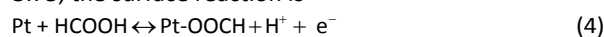
The equilibrium potential for the reaction should shift 59 mV per pH unit. Then, in the RHE scale, it takes place at constant potential. On the other hand, for pH>3.75,

$$Pt + HCOO^- \leftrightarrow Pt\text{-}OOCH + e^- \tag{5}$$
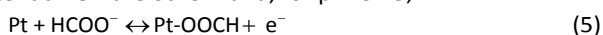
the reaction should occur at constant potential, or shift 59 mV per pH unit in the RHE scale. As can be observed in Fig. 2, the experimental results follow these relationships. For pH<3.75 the onset potential is constant in the RHE scale, whereas for pH>3.75 the onset shift to higher values, although with a smaller shift than that predicted by equation (5). As will be shown later, this smaller shift can be due to the effect of the electrode charge in the reaction rate and/or adsorption processes. The activation energy for the reaction at different pH values have a similar behavior to that observed in 0.1 M $HClO_4$ (Fig. 1). The only significant difference is the lower activation energy at the onset potential for higher pH values.

All these experiments suggest that solution formate is the active species in the reaction, or at least, that one proton has been exchanged in the reaction mechanism of the active intermediate before the rds. Thus, equation (1) should include the concentration of the active species according to

$$j \propto k \exp\left(\frac{\alpha FE}{RT}\right)\theta_A\left(1-\theta_A\right)c_{HCOO^-} \tag{6}$$

Or, if the acid constant of formic acid (K_a) is used, the equation can be expressed as a function of the proton and formic acid concentration:

$$j \propto k \exp\left(\frac{\alpha FE}{RT}\right)\theta_A\left(1-\theta_A\right)c_{HCOO^-} =$$
$$= kK_a \exp\left(\frac{\alpha FE}{RT}\right)\theta_A\left(1-\theta_A\right)\frac{c_{HCOOH}}{c_{H^+}} \tag{7}$$

Direct path DFT calculations. To gain insight into the direct path mechanism of FAOR on platinum different DFT calculations have been carried out on the Pt(100) surface (the one giving rise to the highest currents). The aim was to search for the conditions under which preadsorbed species assist the adsorption of formate in a favorable configuration to yield CO_2 by means of the C—H bond cleavage. First, under neutral charge conditions, it has been found that solvated formic acid is favorably adsorbed on this surface, at top position, by ca. 0.12 eV. Moreover, as can be observed in Fig. 3A, a relatively short hydrogen bond (ca. 1.64 Å) is formed between an explicit water molecule and the O—H group of the adsorbate, as a result of the adsorption process. At the same time, the O—H bond of this group rests elongated with respect to the length that the O—H bond of the solvated formic acid molecule presents in the bulk, from ca. 1.02 to ca. 1.04 Å. This observation suggests that, as an effect of the adsorption process, the adsorbed formic acid has a higher acid constant than in the bulk, favoring its deprotonation toward the solution to yield adsorbed formate. Moreover, it is verified that, under positive charge conditions (those generated when the potential is made more positive) this effect is considerably augmented. Therefore, the identified acidification effect, as a consequence of the adsorption process, relativizes the disjunctive between formic acid and formate as the species

from which FOAR is initiated. From both, formic acid and formate in solution, adsorbed formate is readily obtained, with quantitative details depending on the pH and on the potential. Thus, in any case, adsorbed formate is the key species to consider, in complete agreement with the experimentally derived insights, which indicates that one proton has been exchanged prior to the rate determining step.
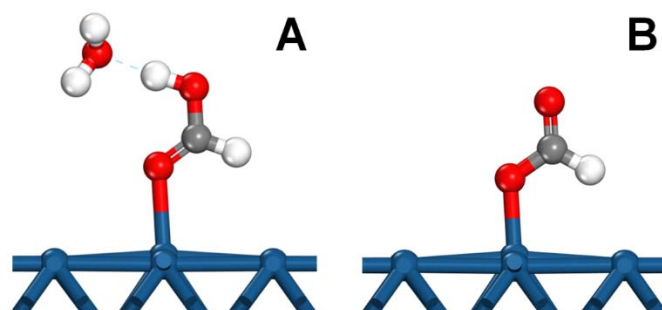

Fig. 3. Adsorbate configurations found at top position on the Pt(100) surface, using a continuous solvation model: A) Solvated formic acid. B) Formate in monodentate form. Color code for atoms: Pt: blue; carbon: grey; oxygen: red and hydrogen: white.

It has been also found that, under neutral charge conditions, formate is favorably adsorbed on the Pt(100) surface, at top position, adopting the monodentate configuration displayed in Figure 3B. The relevance of this configuration can be initially established by means of determining its stability, with respect to an eventual desorption process, which has been estimated to be at least in the order of ca. 1.0 eV. Moreover, it has been also found that, from the displayed monodentate adsorbed formate configuration, the C—H bond can be cleaved, with the aid of a surface site, giving rise to a dehydrogenation process which presents virtually no barrier. Therefore, at this point, it could seem that the direct path mechanism of FAOR has been completely elucidated.

However, nothing is further from reality. It is known that formate can be strongly adsorbed on platinum adopting the bidentate configuration, with the two oxygen atoms bonded to the surface. In fact, it has been calculated that, for the same surface model originating the Fig. 3B, the bidentate adsorbed formate configuration is even ca. 0.70 eV more favorable than the monodentate displayed one, that is the binding energy of adsorbed formate in the bidentate configuration (fig. 4) is close to 1.7 eV. Moreover, DFT-based molecular dynamic simulations show that monodentate adsorbed formate on platinum can easily rotate around the proximal oxygen atom within the plane defined by the adsorbate. At the same time it moves toward the adjacent platinum atom, around the axis defined by the Pt—O bond, and around the axis defined by the adjacent O—C bond. Thus, starting from the clean surface, if the formation process of monodentate adsorbed formate is not followed immediately by the C—H bond cleavage, the adsorbate can evolve to the much more favorable bidentate form. In fact, the energy released during the monodentate phase of the process would excite the described rotation modes, increasing the probability of resting in the much more favorable bidentate form. The problem is that the way in

which the C—H bond cleavage could take place from adsorbed formate in bidentate form does not result obvious. Fortunately, the discussed experimental evidences suggest that preadsorbed species could facilitate the adsorption of formate in the favorable configuration for its complete oxidation.

Thus, to better understand the way in which preadsorbed species could favor the formate adsorption in monodentate form, formate adsorption inside the pocket of preadsorbed formate displayed in Fig. 4 has been also investigated, both under neutral and positive charge conditions. It has been found that formate can be adsorbed inside the pocket adopting the monodentate configuration displayed in Figure 4. The stability energy for this species is ca. 0.5 eV. It has been also verified that, from the displayed configuration, the C—H bond can be cleaved with the aid of the adjacent surface site virtually without barrier. Moreover, it has been also observed that, inside the pocket, the bidentate adsorbed formate configuration is much less favorable with respect to the monodentate one than outside the pocket. However, the most important finding is that, inside the pocket, the rotation modes enabling the transition from the monodentate adsorbed formate to the bidentate form are completely obstructed. Therefore, inside the pocket, the C—H bond cleavage from monodentate adsorbed formate is guaranteed. The preadsorbed formate occupying the longitudinally adjacent site to the one on which monodentate formate is adsorbed inhibits the rotation of the monodentate one around its proximal oxygen atom. Moreover, the parallel preadsorbed formate species inhibit the rotation of the monodentate one around the Pt—O bond. Finally, with these rotation modes inhibited, the transition from the monodentate to bidentate form requires rotation around the C—O bond passing through a plane normal to the parallel planes defined by the preadsorbed formate species, which, inside the pocket, is not possible. Previous DFT calculations about FAOR have tried to estimate activation barriers for the reaction.[49, 50] However, the calculated barriers were higher than those measured experimentally, which suggested that a crucial factor was omitted in the model. According to the present results, a missing element is probably the presence of adsorbed formate.

To explain reactivity differences among different surfaces, it should be considered that adsorption processes are not static. Radiotracer studies demonstrate that species are continuously exchanged between the solution and the adsorbed layer.[51] So, formate species are continuously adsorbing and desorbing from the surface electrode. Thus, formate oxidation is taking place during this dynamic adsorption-desorption process, and it is clear that, the more intense is the process of exchange, the higher number of species can react on the surface. Bidentate formate on Pt(111) is adsorbed in a potential window of ca. 0.4 V. However, anions and hydrogen on Pt(100) are competitive adsorption processes that take place in a narrow potential window. Therefore, on the Pt(100) surface, the process is faster, the exchange more intense, the total

number of involved species higher and, as a result, higher currents are measured.
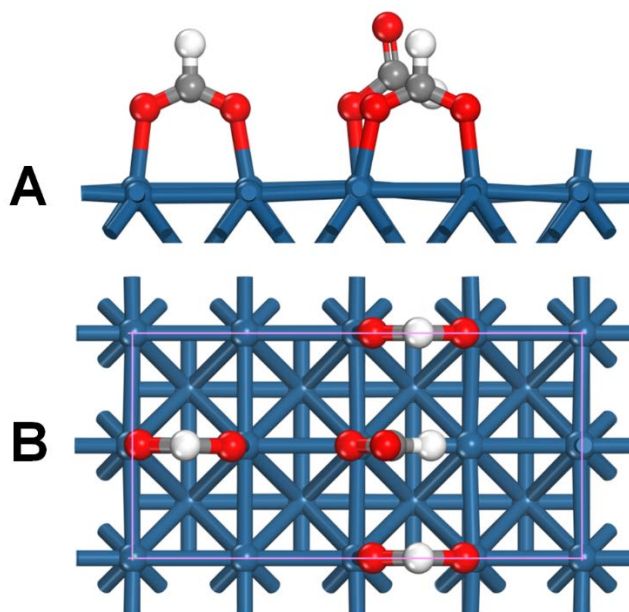
Fig. 4. Monodentate adsorbed formate inside a pocket of preadsorbed bidentate formate on the Pt(100) surface. A) Side view. B) Top view. Lattice is highlighted in magenta. Color code for atoms: Pt: blue; carbon: grey; oxygen: red and hydrogen; white.

Finally, to explore the effect that electrode potential and pH could have on the direct path mechanism of FAOR on platinum, charge was considered in the model. On the one hand, electrode potential changes imply interfacial charge changes. On the other hand, when the pH of the solution changes, the onset of the reaction occurs at a different interfacial charge. So, for instance, as the pH increases, the reaction takes place in a potential window in which the surface has a diminishing positive charge. It has been found that, the bidentate adsorbed formate stability, with respect to the monodentate configuration, increases from 0.70 to 0.89 eV, when one electron is removed from the model. This result suggests that, as the pH increases, the transformation between the bidentate and the reactive form is more favorable, which could explain why at pH>4 the onset potential shift less than 59 mV in the RHE scale.

In short, the acidification effect that formic acid experiences because of its adsorption process diminishes the relevance of the discussion between formic acid and formate as the species from which FOAR would be initiated, highlighting the role of adsorbed formate as the key species to consider. From monodentate adsorbed formate the C—H bond could be cleaved, with the aid of a surface site, virtually without barrier. However, the bidentate form for adsorbed formate is much more favorable than the monodentate one. Under low adsorbates coverage conditions, all the rotation degrees of free available to monodentate adsorbed formate are active, increasing the probability of resting in bidentate form. But, the presence of adsorbates near the adsorbed formate decreases the energetic advantage of the bidentate form, with respect to

the monodentate one, and inhibits rotation degrees. Thus, the presence of adsorbates near the adsorbed formate contribute to stabilizing the monodentate form, favoring the complete oxidation. So, the computational results here described suggest that, monodentate, but not bidentate, adsorbed formate is the active intermediate in the direct path of FAOR on platinum, providing an explanation for the experimental evidences. It should be highlighted that in this mechanism bidentate formate is not a mere blocking species, but it helps in the positioning of an adsorbing formate species in the monodentate configuration.

CO formation path.

The CO formation path of FAOR on platinum was first investigated at open circuit. These initial studies demonstrated that the CO intermediate was accumulated on the surface electrode, providing the maximum CO coverages that could be achieved from formic acid.[52, 53] Those CO coverage values were found to be well below the ones obtained when CO was directly adsorbed from the solution.[54] In fact, hydrogen adsorption was still visible on the electrode when the CO coverages were between 0.7-0.8, depending on the electrode, evidencing the presence of free platinum sites.[54, 55] At these CO coverages, CO-CO interactions were even detected by FTIR,[56] an indication of the presence of CO patches randomly distributed on the surface. In any case, the inhibition of the reaction when abundant platinum sites are still available suggests that the CO formation path has steric conditions, requiring adjacent available surface sites to occur. Although differences between single crystal electrodes were observed in these initial results regarding the final CO coverage or the amount of available platinum sites after CO formation,[56-58] there was no indication of significant differences in the CO formation mechanism between the low index planes of platinum.

However, an important difference appeared when the surfaces were modified with adatoms. For the Pt(100) electrode, the adatom acted as a third body inhibiting the reaction. When adatom coverages were higher than 0.7, the formation of CO was inhibited, in agreement with the observed behavior for the unmodified surface.[55] However, the Pt(111) surface modified by bismuth led to very different results.[54, 59] Trace amounts of bismuth deposited on this electrode were able to inhibit completely the formation of CO from formic acid. This result, which was initially very difficult to explain, was understood when stepped surfaces with (111) terraces were studied. On these stepped surfaces, bismuth is preferentially adsorbed on step sites and, when the deposition process is carefully controlled, decorated stepped surfaces can be obtained before deposition on the terrace occurs.[60] For the decorated surfaces, it was found that the CO formation path was completely inhibited.[61-63] Thus, the CO formation path on

the stepped surfaces takes place only on the steps but not on the terraces. These conclusions allowed to explain the behavior of the Pt(111) electrode. From formic acid, CO is formed on this surface exclusively on defects. And, given that the initial stages of the adatom deposition cover the defects, trace amounts of the adatom are only required to inhibit completely the CO formation. This example illustrates the importance of the defects in reactivity. Although the presence of defect sites in high quality Pt(111) electrodes is well below 1%, processes taking place on these sites could eventually alter the global reactivity of the surface, which highlight the convenience of conducting studies on well-defined single crystal electrodes in electrocatalysis.

Pulsed voltammetry confirmed the negligible CO formation rate for the whole of the potential range on the Pt(111) electrode.[45] Moreover, it was also observed that, on the Pt(100) and different stepped surfaces, CO can be produced from formic acid, in a narrow potential window (ca. 150-200 mV), which was centered around the corresponding potential of zero total charge (pztc).[25, 45] The pztc is the potential value for which the total charge transferred as a result of adsorption processes on the surface is zero. Since hydrogen and anions have, respectively, positive and negative electrosorption valencies,[64] both hydrogen and anions should be present on the surface at pztc at coverage values related with the ratio of the respective electrosorption valencies. Thus, for the Pt(100) surface, the pztc is located in the region where hydrogen and anions are simultaneously adsorbed form the electrolyte. Moreover, on the stepped surfaces with (111) terraces, the maximum CO formation rate is obtained for the local pztc corresponding to the step site, when hydrogen and probably anions are present on the step. Thus, as a conclusion, the CO formation path occurs in a potential window where the adsorption of hydrogen and anions are both favorable, but no one of these adsorption reactions dominate over the other one.

When the CO formation and direct path reaction rates are compared, insights about the relative importance of the undesired path of FAOR can be obtained. In order to make an easy comparison, the CO formation rates and the direct path currents (intrinsic activity) have been transformed into turnover frequencies. So, for the Pt(100) electrode in 0.1 M $HClO_4$ + 0.1 M HCOOH, the maximum intrinsic activity is ca. 45 mA cm^{-2}, which is equivalent to a turnover frequency of 107 molecules s^{-1} Pt site^{-1}. On the other hand, for the CO formation path the turnover frequency is equivalent to 7 molecules s^{-1} Pt site^{-1}, which is 15 times smaller than that for the direct path. This large difference suggests that the CO formation path on this electrode could be considered as a minor side reaction. However, due to the CO accumulation effect on the surface, this side reaction determines the electrode reactivity, highlighting the importance of the side reactions.
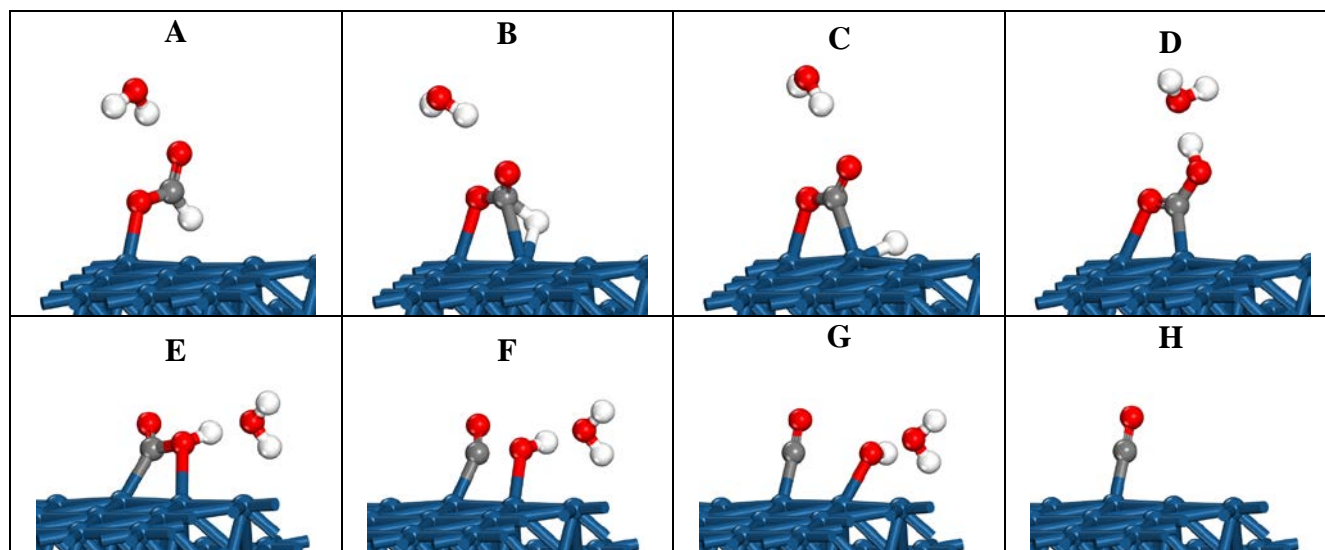
ARTICLE

Fig. 5. States (**A**, **C**, **D**, **G** and **H**), pseudo states (**E**), and transition states (**B** and **F**) involved in the proposed CO formation mechanism. See text for complete details. Color code for atoms: Pt: blue; carbon: grey; oxygen: red and hydrogen: white.

As aforementioned, the reaction rate measured for (111) terraces is negligible, that is, it is well below the sensitivity of the technique used. For the Pt(111) electrode, the intrinsic activity is 2.5 mA cm^{-2}, which is equivalent to 5.2 molecules s^{-1} Pt site^{-1}. Thus, if the turnover ratio between the direct path and the CO formation path were similar to the one calculated for the Pt(100) surface, a CO formation reaction rate on Pt(111) of ca. 0.32 s^{-1} would have been expected. Given that the sensitivity of the pulsed voltammetry for the CO formation rate is ca. 0.005 s^{-1}, it can be concluded that the CO formation reaction on the Pt(111) electrode is even more difficult.

Finally, reaction rates for stepped surfaces depended on the step density. The measured values for the CO formation rate constant for the Pt(13,12, 12), Pt(776) and Pt(554) were 0.5787, 1.1041 and 1.6841 s^{-1}, respectively.[45] These surfaces have a monoatomic (110) steps on (111) terraces, which has 15, 13 and 9 atomic rows, respectively. When these values are transformed into turnover frequencies and taking into account that the reaction only takes place on step sites, a value of 15±1 molecules s^{-1} Pt site^{-1} is obtained for all the surfaces. This value implies that the (110) step sites on the (111) terrace are even more active than the (100) sites. However, in spite of this, their effect on the reactivity of the stepped surfaces is smaller than that observed for the Pt(100) electrode, because the lower number of sites capable of producing CO.

Activation energies for the CO formation path have been also estimated.[21] Although the actual values are different from those obtained for the direct path, the shape of the curves is essentially the same, which indicates that both paths share common steps and influences of the adsorbed anions. The above described experimental evidences and implications provide valuable insights about the CO formation path of FAOR on platinum, such as which the most active surface is, where CO is formed on stepped surfaces, or which the adsorbates are available to the reaction. However, a detailed mechanism for

the reaction, consistent with the whole of these evidences, has not yet been described.

CO formation path DFT calculations. To further investigate the CO formation path of FAOR on platinum, searching for the mechanism, DFT calculations have been carried out on different models of low index and stepped surfaces of platinum. Considering that the experimental evidences suggest that both the direct path and the CO formation path share common steps, and that the previously discussed experimental and computational results point to monodentate adsorbed formate as the specie from which FAOR on platinum is initiated, adsorbed formate, in monodentate form, was fixed as the reactant of the reaction. From this starting point, a plausible mechanism was envisioned, for which the energetic was estimated on three different platinum surfaces: two low index surfaces (Pt(111) and Pt(100)) and one stepped surface (Pt(553)). The idea is to stablish the verisimilitude of the proposed mechanism by the way in which the whole of the obtained computational results is capable of explain the whole of the available experimental evidences about the CO formation path of FAOR on platinum.

It can be argued that, under any conceivable mechanism, the C—H bond should be broken, and that the adsorption mode should change from a Pt—O to a Pt—C binding mode. Our proposed mechanism for the CO formation path of FAO, is visually described in Figure 5, exemplified on the Pt(553) surface. As a first step in the reaction, it is proposed that monodentate adsorbed formate (Figure 5A) dehydrogenates towards the surface, while it changes to a bidentate configuration in which the C atom rests also bonded to the surface (Figure 5C). From this bidentate adsorbed state, the adsorbate evolves to adsorbed carboxylate, for which two different adsorption modes have been considered (Figure 5D, the stable state and E, a pseudo state). Then, from the carboxylate configuration shown in Figure 5E, the C—OH bond is broken on the surface, yielding adsorbed CO and OH (Figure

5G). Finally, OH is desorbed to form water in the final step of the mechanism (figure 5H). The additional states, displayed as figures 5B y F, are the transition states involved in the process: that corresponding to the dehydrogenation process, and that corresponding to the cleavage of the C—OH bond.

Assuming the above described mechanism, the energetics of the different steps of reaction on the Pt(100), Pt(111) and Pt(553) surfaces have been estimated, including the redox potential effects, as indicated by the presence of hydrogen and water molecules. The clean surface and a hydrated formic acid molecule have been used as energy reference, since this is the starting point of the reaction. In Figure 6, it can be identified that, at 0 V vs. RHE, the most difficult step in the reaction is

Moreover, the evolution of the energy profiles with the electrode potential explains why the reaction occurs only in a narrow potential window (figure 7). Although in the global reaction for the path no electrons are exchanged, so that the energetics of the reactants and the final adsorbed CO state are potential independent, the rest of steps are affected by the electrode potential. The initial step, which leads to the adsorption of formate, is an oxidation reaction, whereas the final step, in which OH is desorbed to the solution, is a reduction step. At 0 V vs RHE, the reaction is unlikely due to the high barrier for the first steps. However, as the potential increases, the barrier for the initial step diminishes, favoring the formation of CO. In fact, the calculated energetics of the
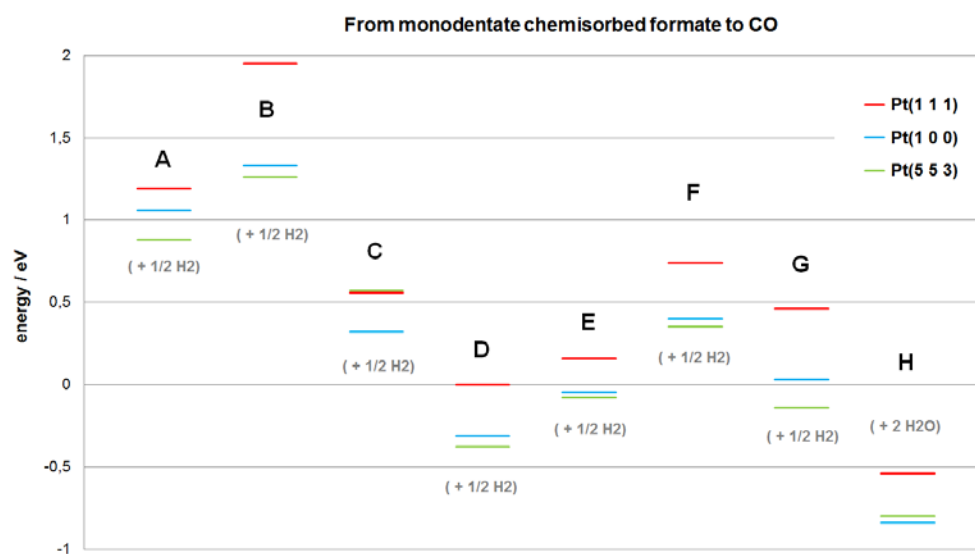

Fig. 6. Energetics of the states, pseudo states, and transition states involved in the proposed CO formation mechanism (see figure 5), estimated on different platinum surfaces at 0 V vs RHE. The values corresponding to the low index Pt(111) and Pt(100) surfaces are show in red and blue, respectively, meanwhile those corresponding to the Pt(553) stepped surface are displayed in green.

the transformation from monodentate adsorbed formate to the bidentate fragment, implying the dehydrogenation. In fact, this first step is the rds. From that point, the total energy of the system diminishes in every step, with the only exception of the process that leads to the cleavage of the C—OH bond, which has small activation energy. The calculated energies for the different surfaces shows clearly that the reaction on the Pt(111) surface has significant higher activation energy than on the other two electrodes. On the Pt(100) and Pt(553) surfaces, the energies of the different configurations are similar, but the barriers are, in general, somehow smaller for the Pt(553) surface. These results agree completely with the experimental data, which indicates that the rates for CO formation path on the Pt(111) electrode are negligible, whereas for the other two surfaces the rates are similar.

adsorption step follows qualitatively the experimentally observed behavior, Pt(553)>Pt(100)>Pt(111) from most to less favorable, which agrees with the observed behavior for the adsorption of anions. As the potential is more positive, the barrier for these steps diminishes to accessible values with the only exception of the Pt(111) electrode. For this electrode, even at 0.6 V the barrier is still very large (1.34 eV to reach the transition step of figure 7B), which implies that the reaction is still very unfavorable. For the other two electrodes, the initial steps become favorable. However, the final desorption of OH, which is a reductive step, becomes a thermodynamically unfavorable step at 0.6 V, inhibiting the process. Thus, only around 0.3 V the reaction is favorable, in agreement with the experimental results.

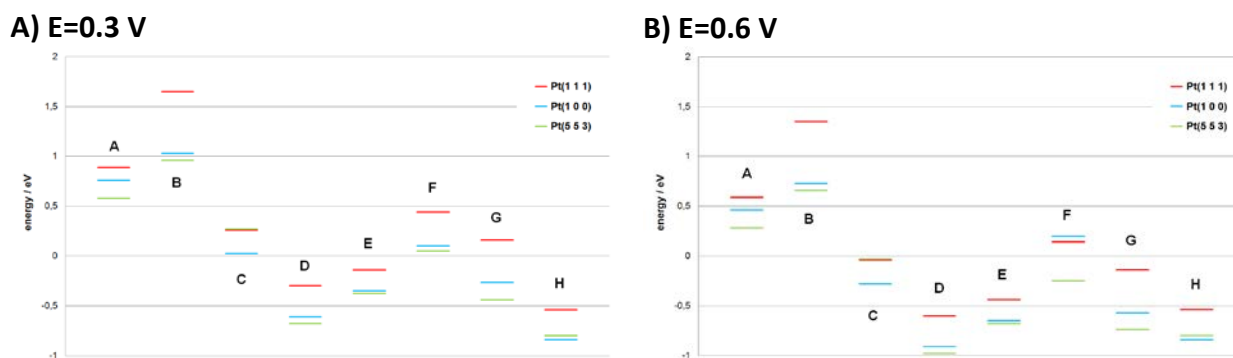## A) E=0.3 V   ## B) E=0.6 V

Fig. 7. Energetics of the states, pseudo states, and transition states involved in the proposed CO formation mechanism (see figure 5), estimated on different platinum surfaces at A) 0.3 V and B) 0.6 V vs RHE. The values corresponding to the Pt(111), Pt(100) and Pt(553) surfaces are show in red, blue and green, respectively.

It should be highlighted that a quantitative agreement between DFT and experimental results is very difficult to achieve. Adsorbed species, their coverages and electrode charge are, all of them, coupled factors, which depend, in turn, on the pH and on the electrode potential. Thus, incoming formic acid molecules face different real conditions, which are difficult to simulate. However, the proposed mechanism for the CO formation path on platinum, and the results reported here can qualitatively explain the experimental results. As aforementioned, on the one hand, the barriers are always very high on Pt(111) electrode, so that the reaction rate is negligible. On the other hand, for the Pt(100) and Pt(553) barriers are accessible in the central potential region. Moreover, adsorbed OH and H are involved in different steps. If the electrode potential is very negative, adsorbed hydrogen is very stable and thus the formation of the carboxylate is unfavorable. However, at very positive potentials OH will not desorb from the surface. Thus, the best window for the reaction is where the energetics for adsorbed H and OH, are similar, that is in the region around the pztc.

Conclusions

Forty years of research about the formic acid oxidation on platinum have consolidated that the reaction takes place under a dual path mechanism model, that the direct path proceeds through an active intermediate, or that the other path give rise to adsorbed CO. However, different aspects of the reaction, such as, the species from which the oxidation processes is initiated, the nature of the true active intermediate or the elucidation of the formation mechanism of CO, remain still controversial. As a result, a complete a detailed mechanism explaining all the available evidences of FAOR on platinum have not been yet described. Here, using a combined experimental and computational approach, the most important outstanding issues about FAOR on platinum have been addressed and, as a conclusion, a complete a detailed mechanism for the reaction has been proposed capable of explaining even pH, surface structure and electrode potential effects.

On the one hand, it has been found that adsorbed formic acid has a higher acid constant than in solution, which suggests that adsorbed formate can be originated not only from formate but also from formic acid, highlighting the role of adsorbed formate as the key species of the reaction. Additionally, it has been also found that two adsorbed formate configurations are relevant: The monodentate and the bidentate adsorption modes. Moreover, adsorbed formate can swing between both of them, being the bidentate form the most favorable. However, it is the monodentate form the one that leads to the complete oxidation to CO_2. Therefore, the bidentate form is dominant under low coverage of adsorbate conditions, as FTIR results indicate. But, at intermediate coverages, the presence of adjacent adsorbates inhibits the transition from monodentate formate to the most stable bidentate form, favoring the complete oxidation to CO_2 in a virtually barrierless process. The described mechanism explains the experimental relationship between adsorbed formate coverages and oxidation currents for the platinum electrodes.

On the other hand, the starting point of the CO formation mechanism would be also monodentate adsorbed formate. During the transition between the monodentate and the bidentate forms, both atoms of the C—H bond could eventually interact simultaneously with the surface, giving rise to a dehydrogenation process in which the C atom rests bonded also to the surface. This kind of event is improbable on the Pt(111) surface, but much more, and similarly, probable on the low index Pt(100) and the stepped Pt(553) surfaces. From this last configuration, the adsorbed fragment evolves to carboxylate, from which C—OH bond is cleaved with the aid of and adjacent atom of the surface. This mechanism would explain differences in reactivity among different surfaces of platinum and why the formation of CO occurs in a narrow potential window around the local pztc of the surface site.

Conflicts of interest

There are no conflicts to declare.

ARTICLE Journal Name

Acknowledgements

References

1. V. S. Bagotzky, Y. B. Vassiliev and O. A. Khazova, *J. Electroanal. Chem.*, 1977, **81**, 229-238.
2. B. Beden, A. Bewick and C. Lamy, *J. Electroanal. Chem.*, 1983, **150**, 505-511.
3. A. Capon and R. Parsons, *J. Electroanal. Chem.*, 1973, **45**, 205-231.
4. A. Capon and R. Parsons, *J. Electroanal. Chem.*, 1973, **44**, 1-7.
5. O. Wolter, J. Willsau and J. Heitbaum *Journal of Electrochemical Society*, 1985, **132**, 1635-1638.
6. J. Willsau and J. Heitbaum, *Electrochim. Acta*, 1986, **31**, 943-948.
7. Y. X. Chen, A. Miki, S. Ye, H. Sakai and M. Osawa, *J. Am. Chem. Soc.*, 2003, **125**, 3680-3681.
8. G. Samjeske and M. Osawa, *Angew. Chem. Int. Ed.*, 2005, **44**, 5694-5698.
9. A. Cuesta, G. Cabello, C. Gutierrez and M. Osawa, *Phys. Chem. Chem. Phys.*, 2011, **13**, 20091-20095.
10. A. Cuesta, G. Cabello, M. Osawa and C. Gutiérrez, *ACS Catal.*, 2012, **2**, 728-738.
11. Y. X. Chen, M. Heinen, Z. Jusys and R. J. Behm, *Langmuir*, 2006, **22**, 10399-10408.
12. Y. X. Chen, M. Heinen, Z. Jusys and R. B. Behm, *Angew. Chem. Int. Ed.*, 2006, **45**, 981-985.
13. Y. X. Chen, M. Heinen, Z. Jusys and R. J. Behm, *ChemPhysChem*, 2007, **8**, 380-385.
14. J. Joo, T. Uchida, A. Cuesta, M. T. M. Koper and M. Osawa, *J. Am. Chem. Soc.*, 2013, **135**, 9991-9994.
15. J. Joo, T. Uchida, A. Cuesta, M. T. M. Koper and M. Osawa, *Electrochim. Acta*, 2014, **129**, 127-136.
16. S. Brimaud, J. Solla-Gullon, I. Weber, J. M. Feliu and R. J. Behm, *ChemElectroChem*, 2014, **1**, 1075-1083.
17. J. V. Perales-Rondón, S. Brimaud, J. Solla-Gullón, E. Herrero, R. Jürgen Behm and J. M. Feliu, *Electrochim. Acta*, 2015, **180**, 479-485.
18. J. Clavilier, R. Parsons, R. Durand, C. Lamy and J. M. Leger, *J. Electroanal. Chem.*, 1981, **124**, 321-326.
19. R. R. Adzic, A. V. Tripkovic and W. E. O'Grady, *Nature*, 1982, **296**, 137-138.
20. A. Ferre-Vilaplana, J. V. Perales-Rondon, J. M. Feliu and E. Herrero, *ACS Catal.*, 2015, **5**, 645-654.
21. J. V. Perales-Rondón, E. Herrero and J. M. Feliu, *J. Electroanal. Chem.*, 2015, **742**, 90-96.
22. J. Clavilier, D. Armand, S. G. Sun and M. Petit, *J. Electroanal. Chem.*, 1986, **205**, 267-277.
23. C. Korzeniewski, V. Climent and J. M. Feliu, in *Electroanalytical Chemistry: A Series of Advances*, eds. A. J. Bard and C. Zoski, CRC Press, Boca Raton, 2012, vol. 24, pp. 75-169.
24. N. Garcia-Araez, V. Climent and J. Feliu, in *Mod Asp Electrochem*, ed. C. G. Vayenas, Springer New York, 2011, vol. 51, ch. 1, pp. 1-105.
25. V. Grozovski, V. Climent, E. Herrero and J. M. Feliu, *ChemPhysChem*, 2009, **10**, 1922-1926.
26. B. Delley, *J. Chem. Phys.*, 1990, **92**, 508-517.
27. B. Delley, *Phys. Rev. B*, 2002, **66**, 155125.
28. B. Hammer, L. B. Hansen and J. K. Nørskov, *Phys. Rev. B*, 1999, **59**, 7413-7421.
29. B. Delley, *J. Chem. Phys.*, 2000, **113**, 7756-7764.
30. B. Delley, *Mol. Simul.*, 2006, **32**, 117-123.
31. J. Neugebauer and M. Scheffler, *Phys. Rev. B*, 1992, **46**, 16067-16080.
32. G. Henkelman and H. Jónsson, *J. Chem. Phys.*, 2000, **113**, 9978-9985.
33. J. A. Keith and T. Jacob, *Angew. Chem. Int. Ed.*, 2010, **49**, 9521-9525.
34. H. J. Monkhorst and J. D. Pack, *Phys. Rev. B*, 1976, **13**, 5188-5192.
35. V. Grozovski, F. J. Vidal-Iglesias, E. Herrero and J. M. Feliu, *ChemPhysChem*, 2011, **12**, 1641-1644.
36. A. Rodes, E. Pastor and T. Iwasita, *J. Electroanal. Chem.*, 1994, **376**, 109-118.
37. J. Xu, D. F. Yuan, F. Yang, D. Mei, Z. B. Zhang and Y. X. Chen, *Phys. Chem. Chem. Phys.*, 2013, **15**, 4367-4376.
38. J. V. Perales-Rondon, E. Herrero and J. M. Feliu, *Electrochim. Acta*, 2014, **140**, 511-517.
39. E. Herrero, K. Franaszczuk and A. Wieckowski, *J. Phys. Chem.*, 1994, **98**, 5074-5083.
40. H.-F. Wang and Z.-P. Liu, *J. Phys. Chem. C*, 2009, **113**, 17502-17508.
41. K. A. Schwarz, R. Sundararaman, T. P. Moffat and T. C. Allison, *Phys. Chem. Chem. Phys.*, 2015, **17**, 20805-20813.
42. J. V. Perales-Rondon, A. Ferre-Vilaplana, J. M. Feliu and E. Herrero, *J. Am. Chem. Soc.*, 2014, **136**, 13110-13113.
43. J. Clavilier, *J. Electroanal. Chem.*, 1987, **236**, 87-94.
44. A. Fernández-Vega, J. M. Feliu, A. Aldaz and J. Clavilier, *J. Electroanal. Chem.*, 1991, **305**, 229-240.
45. V. Grozovski, V. Climent, E. Herrero and J. M. Feliu, *Phys. Chem. Chem. Phys.*, 2010, **12**, 8822-8831.
46. V. Grozovski, J. Solla-Gullon, V. Climent, E. Herrero and J. M. Feliu, *J. Phys. Chem. C*, 2010, **114**, 13802-13812.
47. M. T. M. Koper, *Chem. Sci.*, 2013, **4**, 2710-2723.
48. M. T. M. Koper, *Top. Catal.*, 2015, **58**, 1153-1158.
49. M. Neurock, M. Janik and A. Wieckowski, *Faraday Discuss.*, 2009, **140**, 363-378.
50. W. Gao, J. A. Keith, J. Anton and T. Jacob, *J. Am. Chem. Soc.*, 2010, **132**, 18377-18385.
51. M. E. Gamboaaldeco, E. Herrero, P. S. Zelenay and A. Wieckowski, *J. Electroanal. Chem.*, 1993, **348**, 451-457.
52. J. Clavilier and S. G. Sun, *J. Electroanal. Chem.*, 1986, **199**, 471-480.
53. S. G. Sun, J. Clavilier and A. Bewick, *J. Electroanal. Chem.*, 1988, **240**, 147-159.
54. E. Herrero, A. Fernández-Vega, J. M. Feliu and A. Aldaz, *J. Electroanal. Chem.*, 1993, **350**, 73-88.

55. E. Herrero, J. M. Feliu and A. Aldaz, *J. Electroanal. Chem.*, 1994, **368**, 101-108.

56. T. Iwasita, X. H. Xia, E. Herrero and H. D. Liess, *Langmuir*, 1996, **12**, 4260-4265.

57. D. S. Corrigan and M. J. Weaver, *J. Electroanal. Chem.*, 1988, **241**, 143-162.

58. S. C. Chang, L. W. H. Leung and M. J. Weaver, *J. Phys. Chem.*, 1990, **94**, 6013-6021.

59. J. Clavilier, A. Fernández-Vega, J. M. Feliu and A. Aldaz, *J. Electroanal. Chem.*, 1989, **258**, 89-100.

60. E. Herrero, V. Climent and J. M. Feliu, *Electrochem. Commun.*, 2000, **2**, 636-640.

61. M. D. Maciá, E. Herrero, J. M. Feliu and A. Aldaz, *Electrochem. Commun.*, 1999, **1**, 87-89.

62. M. D. Maciá, E. Herrero, J. M. Feliu and A. Aldaz, *J. Electroanal. Chem.*, 2001, **500**, 498-509.

63. M. D. Maciá, E. Herrero and J. M. Feliu, *Electrochim. Acta*, 2002, **47**, 3653-3661.

64. N. Garcia-Araez, V. Climent, E. Herrero, J. M. Feliu and J. Lipkowski, *J. Electroanal. Chem.*, 2005, **582**, 76-84.